

Key Points:

- Interaction of the low-level wind with capes and islands enhances the transfer of energy from the atmosphere to the ocean
- The wind energizes submesoscale cyclonic eddies, enhancing productivity in the Santa Barbara Channel
- Submesoscale cyclonic eddies advect low oxygen, acidic waters beyond the Channel into the broader California Current

Correspondence to:

F. Kessouri,
faycalk@sccwrp.org

Citation:

Kessouri, F., Renault, L., McWilliams, J. C., Damien, P., & Bianchi, D. (2022). Enhancement of oceanic eddy activity by fine-scale orographic winds drives high productivity, low oxygen, and low pH conditions in the Santa Barbara Channel. *Journal of Geophysical Research: Oceans*, 127, e2022JC018947. <https://doi.org/10.1029/2022JC018947>

Received 4 JUN 2022

Accepted 11 NOV 2022

Author Contributions:

Conceptualization: Lionel Renault, James C. McWilliams

Formal analysis: Pierre Damien

Funding acquisition: James C. McWilliams, Daniele Bianchi

Investigation: Pierre Damien, Daniele Bianchi

Methodology: Lionel Renault, Pierre Damien, Daniele Bianchi

Software: Lionel Renault, James C. McWilliams





Supervision: James C. McWilliams

Writing – original draft: Lionel Renault

Writing – review & editing: James C. McWilliams, Pierre Damien, Daniele Bianchi

Bianchi

Enhancement of Oceanic Eddy Activity by Fine-Scale Orographic Winds Drives High Productivity, Low Oxygen, and Low pH Conditions in the Santa Barbara Channel

Fayçal Kessouri^{1,2} , Lionel Renault³ , James C. McWilliams² , Pierre Damien², and Daniele Bianchi² 

¹Southern California Coastal Water Research Project, Costa Mesa, CA, USA, ²Department of Atmospheric and Oceanic Sciences, University of California Los Angeles, Los Angeles, CA, USA, ³University of Toulouse, IRD, CNRS, CNES, UPS, Toulouse, France

Abstract The Santa Barbara Channel is one of the most productive regions of the California Current System. Yet, the physical processes that sustain this high productivity remain unclear. We use a high-resolution physical-biogeochemical model to show that submesoscale eddies generated by islands are energized by orographic effects on the wind, with significant impacts on nutrient, carbon, and oxygen cycles. These eddies are modulated by two co-occurring air-sea-land interactions: transfer of wind energy to ocean currents that intensifies ocean eddies, and a wind-current feedback that tends to dampen them. Here we show that the dampening is overwhelmed by fine scale wind patterns induced by the presence of surrounding capes and islands. The fine-scale winds cause an additional transfer of momentum from the atmosphere to the ocean that energizes submesoscale eddies. This drives upward doming of isopycnals in the center of the channel, allowing a more efficient injection of nutrients to the surface, and triggering intense phytoplankton blooms that nearly double productivity relative to the case without fine-scale winds. The intensification of the doming effect by the wind-curl and submesoscale eddies pumps deep low oxygen, acidic waters to the center of the cyclonic eddies. These eddies are then transported away from the Channel into the California Current, where they impact a wider area along the central coast, with potential ecological consequences. Our study highlights the important role of air-sea-land interactions in modulating coastal processes, and suggests that submesoscale resolving models are required to correctly represent coastal processes and their ecological impacts.

Plain Language Summary Surface waters in the Santa Barbara Channel of California are very rich in phytoplankton, the small algae responsible for photosynthesis in the ocean. This abundance is caused by winds, which pump deep water rich in nutrients to the surface each spring and summer, and by vortices of the size of few tens of km that form in the wake of the Channel Islands. In this study, we use very detailed simulations of the Santa Barbara Channel carried out on supercomputers to show that these vortices become much more intense when they interact with small-scale patterns in the winds, such as strong jets that blow between capes and islands. We show that while the interactions between the surface currents and the atmosphere tend to slow down the vortices, the small-scale winds actually accelerate them, making them stronger. These vortices in turn help pumping more waters rich in nutrients to the surface, fertilizing phytoplankton. This deep water is also poor in oxygen and acidic, and is often transported outside of the Santa Barbara Channel, where it could affect the behavior of marine animals that thrive in more oxygenated and less acidic waters.

1. Introduction

The Santa Barbara Channel (SBC) is part of the California Current System (CCS). It is located in the Southern California Bight, between the Santa Barbara coast and four of the Channel Islands (from west to east: San Miguel, Santa Rosa, Santa Cruz and Anacapa Island, see Figure 1). The center of the channel is characterized by intense phytoplankton blooms in spring and summer (Figures 1a and 1b), when chlorophyll concentrations can exceed 10 mg m^{-3} , generated by wind-driven upwelling (Brzezinski & Washburn, 2011) and recurring cyclonic eddies embedded into a broad cyclonic circulation pattern (Hendershott & Winant, 1996). These intense blooms are likely generated by the interplay of two processes. First, wind-driven upwelling brings deep, nutrient-rich waters to the surface in spring and summer (Brzezinski & Washburn, 2011). Second, recurring cyclonic eddies

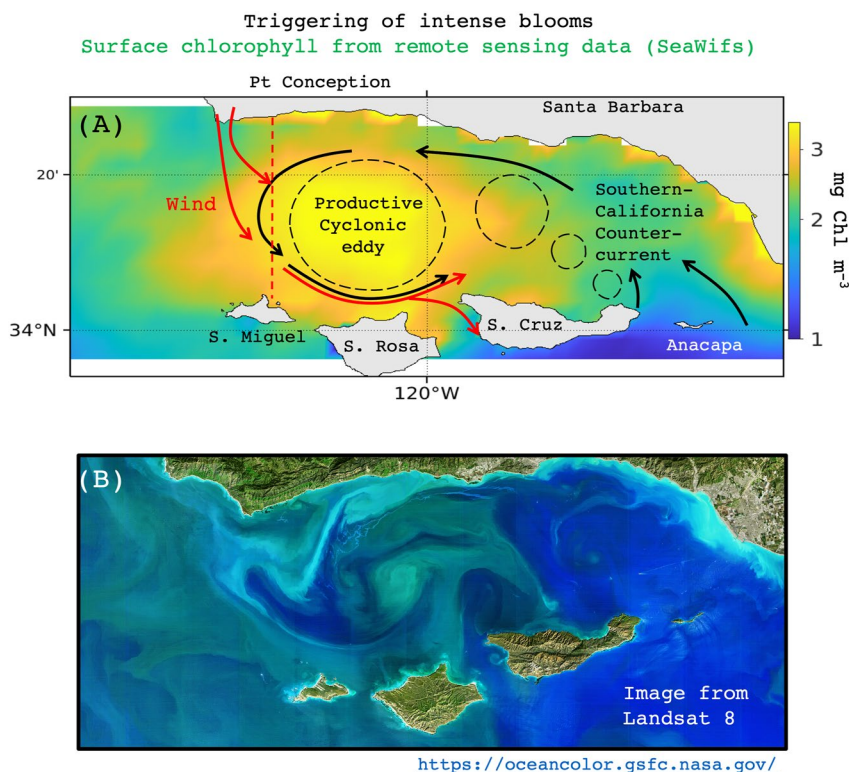


Figure 1. (a) Evidence of recurrent chlorophyll-enriched submesoscale cyclonic eddies in the center of Santa Barbara Channel, based on satellite remote sensing data. The background is seasonally-averaged surface chlorophyll from SeaWiFS between 1997 and 2000. Red arrows show the dominant wind, black arrows the dominant surface ocean currents. (b) false-color image from Landsat8 collected on 1 February 2020 showing a highly productive submesoscale cyclonic eddy near the center of Santa Barbara Channel (source: <https://oceancolor.gsfc.nasa.gov/>).

embedded into a broad cyclonic circulation pattern (Hendershott & Winant, 1996) enhance productivity by lifting isopycnals and increasing nutrient supply near the center of the Channel (Brzezinski & Washburn, 2011).

Eddy activity in this region is generally attributed to the so-called “island mass effect” (Dong & McWilliams, 2007; Doty & Oguri, 1956), that is, generation of cyclonic submesoscale currents (eddies with horizontal scale of 1–10 km and a relative vorticity $[\zeta/f] > 1$; see Section 3.1) that result from the interaction between the islands and the mean current. This interaction drives the emergence of oceanic wakes (Dong & McWilliams, 2007) and intense cyclonic eddies that can destratify the surface ocean (R. M. Caldeira et al., 2005). The island mass effect has been suggested to increase surface turbulence, nutrient supply, and productivity near islands (Messié et al., 2020). In the open ocean, mesoscale and submesoscale eddies can modulate and even trigger phytoplankton blooms (Mahadevan & Archer, 2000; McGillicuddy Jr, 2016). By contrast, in the CCS, mesoscale eddies tend to reduce the overall productivity via the so-called “eddy quenching” effect (Renault, Deutsch, et al., 2016), while submesoscale currents drive a reduction in productivity near the coast, and an increase offshore (Kessouri, Bianchi, et al., 2020). However, the impacts of submesoscale eddies generated by the island mass effect in this region remain poorly understood.

In the past decades, mesoscale air-sea interactions have received growing attention. Satellite observations and numerical models have been used to demonstrate their global ubiquity and effect on surface winds and ocean dynamics (see e.g., D. Chelton, 2001; D. B. Chelton et al., 2004; D. B. Chelton & Xie, 2010; O’Neill et al., 2010; O’Neill, 2012; Ma et al., 2016; Renault, Masson, et al., 2019; Renault, Molemaker, et al., 2016; Renault et al., 2017). At first, attention was essentially given to the thermal feedback, that is, the influence of sea surface temperature on wind, surface stress, and heat fluxes for example, D. B. Chelton et al. (2004, 2007); Minobe et al. (2008); Ma et al. (2016). The feedback of surface currents on the surface stress and overlying winds (current feedback) is an aspect of air-sea interactions that gained subsequent interest (Bye, 1985; Dewar & Flierl, 1987; Duhaut & Straub, 2006; Renault, Marchesiello, et al., 2019; Renault, Molemaker, et al., 2016; Seo

et al., 2016). In the CCS, the current feedback induces a sink of energy from submesoscale oceanic currents to the atmosphere, dampening (sub)mesoscale activity in a process referred to as *eddy killing* (Renault et al., 2018; Renault, Marchesiello, et al., 2019; Renault, Molemaker, et al., 2016).

Fine-scale coastal winds can also influence submesoscale activity (Dong & McWilliams, 2007; Renault, Deutsch, et al., 2016), for example, by altering the characteristics of the undercurrent and thus indirectly modulating the baroclinic and barotropic energy conversion (Chen et al., 2021). Gap winds have also been shown to intensify eddies, for example, as recently shown in the Mediterranean Sea southeast of Crete (Ioannou et al., 2020). In the SBC, the presence of islands and capes generates complex orographic effects, such as wind fans (Winant et al., 1988) and wind wakes (Dong & McWilliams, 2007). These can both enhance the surface wind stress curl, for example, south of the cape at Point Conception where wind stress is intensified southward (Renault, Hall, & McWilliams, 2016). Previous work suggests that wind wakes in this region influence the development of eddies (Dong & McWilliams, 2007), which could potentially counterbalance the *eddy killing* effect by creating a conduit of energy from the atmosphere to the ocean. However, the extent to which the combined effects of air-sea interactions and fine-scale wind modulate eddy strength, productivity and ocean biogeochemistry is still an open question.

The SBC is home to a productive ecosystem that supports valuable marine resources and high biodiversity, and encompasses multiple Marine Protected Areas. For instance, multiple marine mammal species spend at least part of their life cycle near the Channel Islands (Kuhn & Costa, 2014). A better understanding of the interaction between the atmospheric forcing, ocean circulation, biogeochemistry, and productivity is essential to characterize the dynamics of this ecosystem and its response to climatic stressors. For example, ocean warming, oxygen loss, and acidification have been shown to affect the habitat of sentinel species in the CCS, such as anchovies (Howard et al., 2020) and pelagic calcifiers (Bednaršek et al., 2017). Understanding the response of these and other sensitive species requires a characterization of the natural variability in carbon and oxygen and its drivers.

In this study, we show results from two simulations with a submesoscale-resolving ocean physical-biogeochemical model of the SBC. The first, a control simulation run for a period of 4 years, includes fine-scale winds patterns (wind fans and wind wakes) induced by the mainland orography and the islands, and a parameterization of the current feedback (Renault et al., 2020). The second only differs by the absence of fine-scale winds, and was run for a shorter period of 3-month. The simulations are used to investigate the extent to which fine-scale winds can overcome the *eddy killing* effect in the SBC, and the associated impacts on productivity, carbon and oxygen cycles. The rest of the paper is organized as follows. Section 2 describes the model configurations. Section 3.1 explores the energizing effect of high resolution winds on submesoscale eddies. Section 3.2 describes the impacts of eddies on nutrient supply and productivity. Section 3.3 discusses the impacts on oxygen and carbon cycles, and Section 4 concludes the manuscript.

2. Methods

The oceanic simulations are conducted with the Regional Ocean Modeling System, ROMS (Shchepetkin, 2015; Shchepetkin & McWilliams, 2005) coupled to the Biogeochemical Elemental Cycling model, BEC (Moore et al., 2004). BEC is a multi-element (C, N, P, O, Fe, Si) and multiplankton model that includes three explicit phytoplankton functional groups (picoplankton, silicifying diatoms, N-fixing diazotrophs), one zooplankton group, and dissolved and sinking organic detritus. The impacts of calcifying phytoplankton (coccolithophores) on the carbon system are represented implicitly. Two main configurations are enclosed in a coast-wide 4-km resolution simulation (Deutsch et al., 2021; Renault et al., 2021) using offline nesting. A 1-km horizontal resolution configuration (Kessouri, Bianchi, et al., 2020), covering the California coast, and a 300-m horizontal resolution configuration (Kessouri et al., 2021), covering the Southern California Bight (CTRL). Hourly surface momentum, heat, and fresh water fluxes are derived from a 6-km resolution Weather Research and Forecast (WRF; Skamarock & Klemp, 2008) atmospheric simulation (Renault, Hall, & McWilliams, 2016) using bulk formulae (Fairall et al., 2003) modified to include a wind-current coupling parameterization necessary to attain more realistic oceanic submesoscale circulation (Renault et al., 2017, 2020; Renault, Molemaker, et al., 2016). We used the so-called wind-correction approach (Renault et al., 2020) with a coupling coefficient of $s_w = 0.23$ that has been evaluated for the California upwelling in (Renault et al., 2021) (see their Figure 23). The surface stress is therefore estimated using $Ua - (1 - s_w)Uo$. s_w represents the wind adjustment to the current feedback, ignoring it would cause an overestimation of the eddy killing and, thus, a too weak a mesoscale activity.

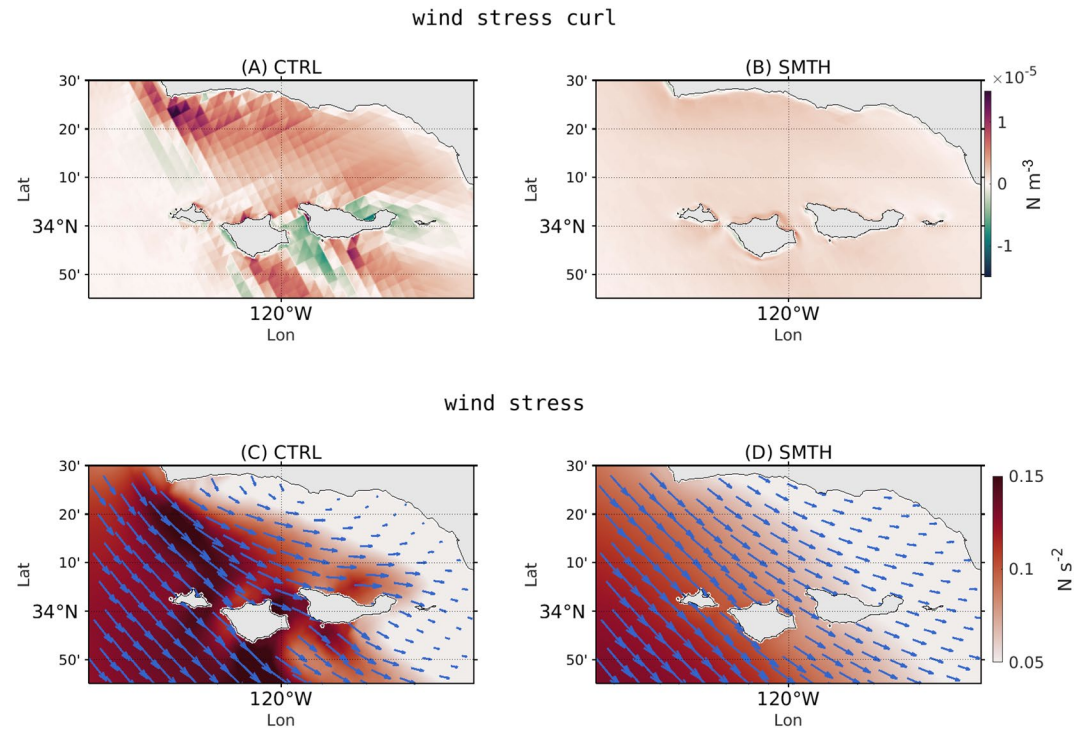


Figure 2. Comparison of summertime (1 June to 31 August 2000) wind stress curl (a–b) and wind stress (c–d) between the SMTH and CTRL simulations. Illustrating the impact of high resolution low-level wind (included in CTRL, but not in SMTH) on submesoscale eddies.

The atmospheric forcing includes fine-scale low-level wind such as island mass effects (Doty & Oguri, 1956) and wind fans (Winant et al., 1988) generated by the numerous capes and mountain ranges in the region (Figure 1). The 1-km model is run for the period 01/1997–12/2007, after a spin-up of 4 years. CTRL is initialized and forced from the 1-km model using the same atmospheric forcing, starting on 01/1997 and ending on 12/2000. A detailed description of the model set up and configuration is presented in Kessouri et al. (2021). We carried out an additional simulation (SMTH) over a 3-month period, initialized from CTRL on 1 June 2000. In this simulation, the 10-m wind used to force the ocean was smoothed using a Whittaker filter (Eilers, 2003) with an equivalent cut-off length scale of ≈ 40 -km. As shown in Figure 2, the smoothed 10-m wind does not represent the wind fan nor the topographic effects of islands on the wind curl (Figures 2a and 2b) and wind stress (Figures 2c and 2d). The smoothed wind field in the SMTH simulation (Figures 2b–2d) is similar to that from commonly-used reanalysis products such as CFSR ($dx = 35$ -km) or NAM ($dx = 12$ -km) as shown in Renault et al. (2021). Like SMTH, these two atmospheric products fail to represent at fine-scale structures close to capes and islands simulated by CTRL. The overall large scale wind strength is similar in both CTRL and SMTH across the domain, except in the southern branch of the islands and the cape of Point Conception.

3. Results

3.1. Energizing of Submesoscale Eddies by Fine-Scale Wind

During the 3-month common simulation period, in CTRL both surface wind stress intensity and curl are characterized by fine scale structures caused by orographic effects along the coastline and the islands (Figures 2c and 2d for wind stress). Over the SBC, the mean surface stress is marked by a southward intensification, with core values of up to 0.2 N s^{-2} . This core is associated with a strong drop-off toward the coast and a mean wind stress curl of $\approx 0.08 \cdot 10^{-5} \text{ N m}^{-3}$. North of San Miguel and Santa Rosa Islands, the surface stress veers eastward, blowing strongly along the northern coast of the islands (Figure 2c). By contrast, SMTH does not represent such a spatial heterogeneity and is characterized by a more uniform wind pattern (Figure 2d). The surface wind stress in SMTH

has a wide and weak drop-off, as revealed by surface stress magnitudes decreasing from 0.1 N s^{-2} offshore to 0.05 N s^{-2} near the coast.

Figures 3a and 3b shows the surface current vorticity averaged over the 3-month common simulation period for both CTRL and SMTH in the center of the Channel (dashed line in Figure 1a). At the eastern entrance of the SBC, the northward flowing Southern California Counter Current meets the Anacapa and Santa Cruz Islands, forming eddies in both simulations. This island mass effect generates submesoscale eddies by barotropic instability (R. M. Caldeira et al., 2005; R. Caldeira et al., 2002; Doty & Oguri, 1956; Messié et al., 2020), and is similar to the cyclonic eddy generation mechanism described by Dong and McWilliams (2007) for Santa Catalina Island, southeast of the Channel. After an eddy with a positive vorticity is formed northeast of the Islands, a cyclonic spiral leaves the Islands to the west. However, comparison of the two simulations reveals that these submesoscale eddies are more vigorous in CTRL relative to SMTH (Figure 3g). On average, the surface relative vorticity (ζ/f) increases by nearly 85%, from 0.26 (maximum of 3.4) in SMTH to 0.48 (maximum of 4.9) in CTRL (compare panels a and b in Figure 3). The most striking difference between the simulations occurs after the formation of the eddies. While in both simulations eddies travel westward through the channel, in CTRL, the presence of fine-scale wind intensifies the eddies, which reach the largest size and most intense vorticity and eddy kinetic energy North of San Miguel and Santa Rosa Islands (Figure 3e). The probability distribution function demonstrates a statistical difference leaning toward more positive values in the CTRL run (Figure 3g). The characteristic shape and location of these eddies compare well with in situ observations (Brzezinski & Washburn, 2011). As shown below, the reduced transfer of energy from the wind to the ocean in SMTH results in weaker eddy kinetic energy (Figure 3f), demonstrating the importance of fine-scale orographic wind patterns on submesoscale oceanic circulation.

The eddy windwork ($F_e K_e$) represents the exchange of momentum between oceanic (sub)mesoscale currents and the atmosphere. A negative $F_e K_e$ indicates a transfer of momentum from an eddy to the atmosphere, and vice versa. Panels c and d in Figure 3 show $F_e K_e$ averaged over the 3-month common period. Consistent with previous work (Renault, Molemaker, et al., 2016), SMTH is characterized by a weak positive $F_e K_e$ on the southern branch of the eddy ($5 \text{ cm}^3 \text{ s}^{-3}$) that is overwhelmed by a large negative $F_e K_e$ on the northern-western branch ($-10 \text{ cm}^3 \text{ s}^{-3}$). The average $F_e K_e$ over the eddy is negative ($-4 \text{ cm}^3 \text{ s}^{-3}$, the largest dashed circle in Figure 1a), revealing a dampening of the eddies by the ocean current feedback on the wind stress. By contrast, in CTRL, the dipole is intensified and shows a strong negative $F_e K_e$ over the northern branch, and a strong positive and wide $F_e K_e$ over the southern branch. Thus, the *eddy killing* is counterbalanced (see the more negative values Figure 3h), resulting in an averaged positive $F_e K_e$ ($3 \text{ cm}^3 \text{ s}^{-3}$), with positive values (up to $30 \text{ cm}^3 \text{ s}^{-3}$ (see large difference in the positive distribution in Figure 3h)) that intensify eddies kinetic energy along the channel (compare e and f in Figure 3). The PDF in (Figure 3i) demonstrates a statistical difference between the runs. The positive values of EKE are two times higher in CTRL.

In summary, submesoscale eddies are first generated by centrifugal, barotropic and baroclinic instabilities in both SMTH and CTRL. Dong et al. (2007) have shown that the three processes play an important role in this system. While traveling through the SBC, in SMTH, these eddies are dampened by the *eddy killing* mechanism, that is, the negative $F_e K_e$. By contrast, in CTRL, the fine-scale wind creates a conduit of energy from the atmosphere to the ocean that overwhelms the *eddy killing* effect. Commonly-used atmospheric reanalysis products, such as CFSR (Renault et al., 2021), do not represent fine-scale wind features and thus would not induce this conduit of energy, similar to the SMTH case (Renault et al., 2021). This is consistent with previous work (Ioannou et al., 2020) that emphasizes the importance of resolving wind jets for the intensification of anticyclonic eddies Southeast of Crete.

3.2. Effects on Nutrients and Phytoplankton Productivity

The concentration of phytoplankton at the location of the eddies in the SBC (the largest dashed circle in Figure 1) is characterized by a strong seasonal cycle that peaks during summer, as shown by chlorophyll values greater than 4 mg m^{-3} (Figure 4d). We hypothesize that intense summertime blooms are driven by coupling between seasonal upwelling and submesoscale vortices: nutrients are brought close to the surface by upwelling (resulting in the seasonal increase in chlorophyll shown by the black line in Figure 4d), and eventually advected into the euphotic zone by submesoscale cyclones (resulting in high-frequency nutrients inputs “spikes” shown by the green line in Figure 4a and peaks in the biomass (Figure 4b)). Accordingly, a weakening of submesoscale cyclonic eddies should cause a decrease in nutrient supply (Figure 4c), chlorophyll concentration (Figure 4d), and net primary production in the Channel. Indeed, the temporal evolution of phytoplankton biomass drastically differs between

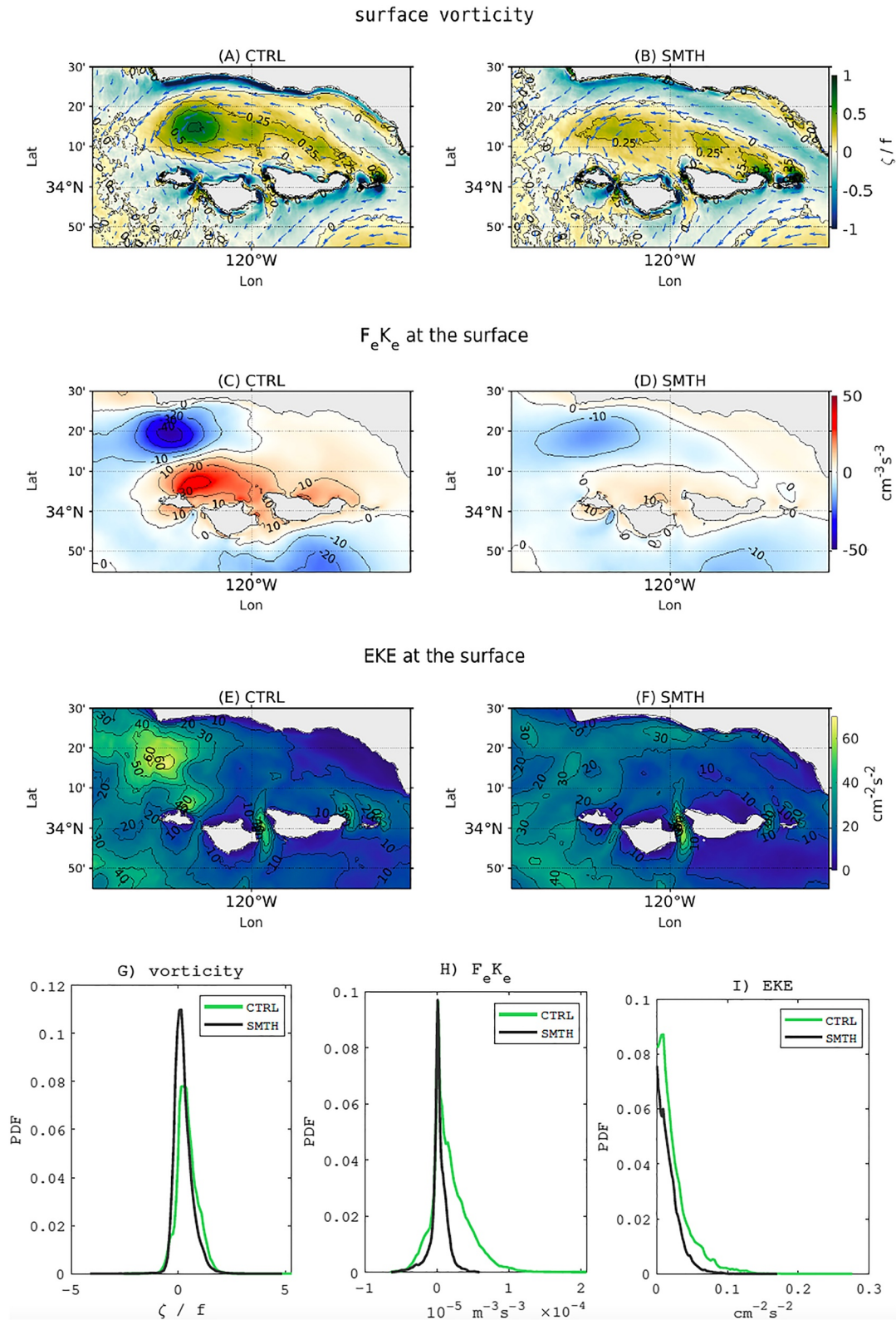


Figure 3.

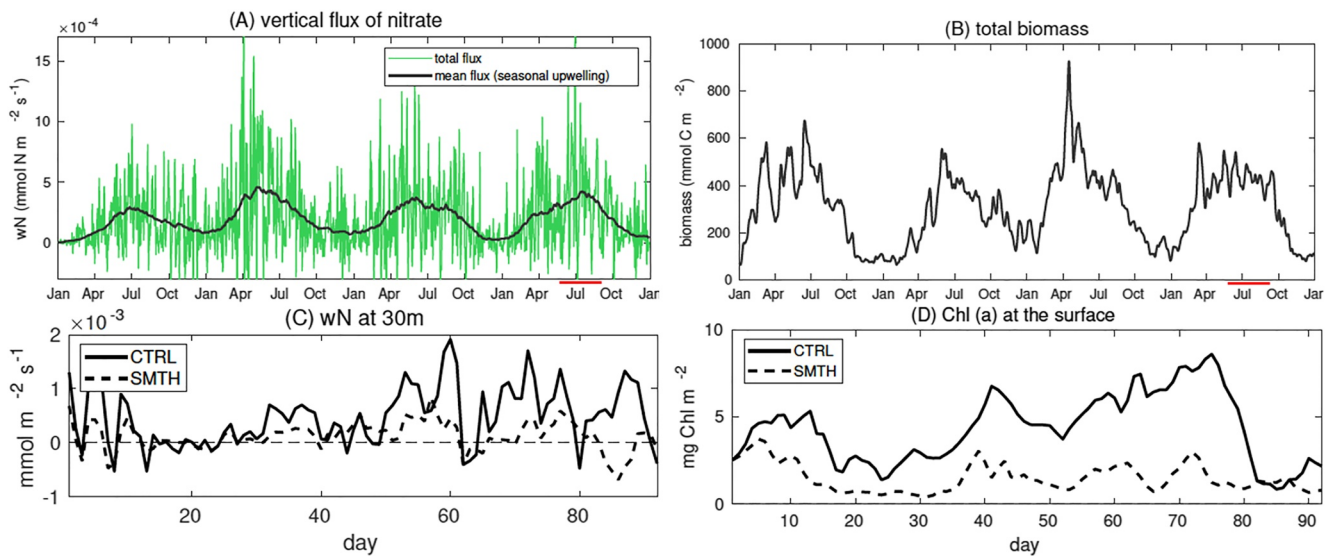


Figure 4. (a) Time series of subsurface vertical flux of nitrate at 50 m depth in CTRL averaged over the Santa Barbara Channel (full area of the maps Figures 5a–5f). In green is the total flux in CTRL, and in black is the mean flux, calculated after Reynolds decomposition with a 90 days moving filter. (b) Time series of the vertically integrated biomass [0–50 m depth] of phytoplankton in average over Santa Barbara Channel. (c) Time series of the vertical flux of nitrate in CTRL (solid line) and SMTH (dashed line) between 1 June and 31 August 2000 (red line in a–b). (d) similar to (c) but for the surface chlorophyll concentration.

the CTRL and SMTH simulations. In the middle of the Channel, CTRL is characterized by concentrations of more than $10.5 \text{ mg Chl m}^{-3}$ ($4.3 \text{ mg Chl m}^{-3}$ on average) whereas SMTH never exceeds $4.5 \text{ mg Chl m}^{-3}$ (only $1.5 \text{ mg Chl m}^{-3}$ on average). As revealed by the temporal evolution in Figure 4d, during summer 2000, surface chlorophyll nearly collapses in SMTH.

Analysis of the nutrient distribution indicates a reduction in nutrient supply when submesoscale eddies are weakened by lack of fine-scale winds. In CTRL, more vigorous submesoscale eddies drive a stronger upward doming of isopycnals (Figures 6a and 6b), causing them to outcrop near the center of the Channel (Figures 5a and 5b), and facilitating nutrient delivery to the surface (Figure 4c). In CTRL, the average nitrate concentration in the upper ocean exceeds 20 mmol m^{-3} , with a maximum of 29 mmol m^{-3} at 50 m (Figure 5a). In SMTH, doming of isopycnals is greatly reduced and surface nutrients stabilize at around 15 mmol m^{-3} (Figure 5b).

As a result of the greater nutrient supply, surface net primary production at the center of the Channel is higher in CTRL (Figure 5c), reaching values in excess of $15 \text{ mmol C m}^{-3} \text{ d}^{-1}$, while in SMTH it remains around $5 \text{ mmol C m}^{-3} \text{ d}^{-1}$ (Figure 5d).

Analysis of vertically integrated net primary production (Figures 5e and 5f) and of a cross section of net primary production through the Channel (Figures 6a and 6b) reveals a potential trade-off between surface and subsurface productivity in the two simulations. While in CTRL most of the productivity occurs near the surface, in SMTH it is localized in a subsurface productivity maximum between 10 and 25 m. However, while a shift to deeper production partially compensates for the lower surface production in SMTH, the vertically integrated production remains approximately 30% smaller than in the CTRL case (Figure 6c).

The relationship between net primary production and nutrient supply suggests that both upwelling and submesoscale eddies are necessary to support high productivity in the SBC. The importance of upwelling is supported by the temporal evolution of the nitrate flux to the upper layer, which shows seasonal pulses each spring and summer (Figure 4a). A similar dynamic characterizes the total phytoplankton biomass (Figure 4b), and nutrients flux and

Figure 3. Comparison of summertime (1 June to 31 August 2000) ocean circulation characteristics between the CTRL (a, c, e) and SMTH (b, d, f) simulations. Color contours show surface relative vorticity (ζ/f) in (a) and (b); eddy windwork ($F_e K_e$) in (c) and (d); and surface eddy kinetic energy in (e) and (f). Blue arrows in (a) and (b) show surface currents. (g, h, i) are the probability distribution functions (PDFs) of surface vorticity, eddy wind work and surface eddy kinetic energy in both simulations; green line for CTRL run and black line for SMTH run. The PDFs are calculated from daily outputs during summer-time in the center of the eddy (dashed circle in Figure 1a). They demonstrate the statistical difference in the distribution of the surface ocean circulation between the two simulations.

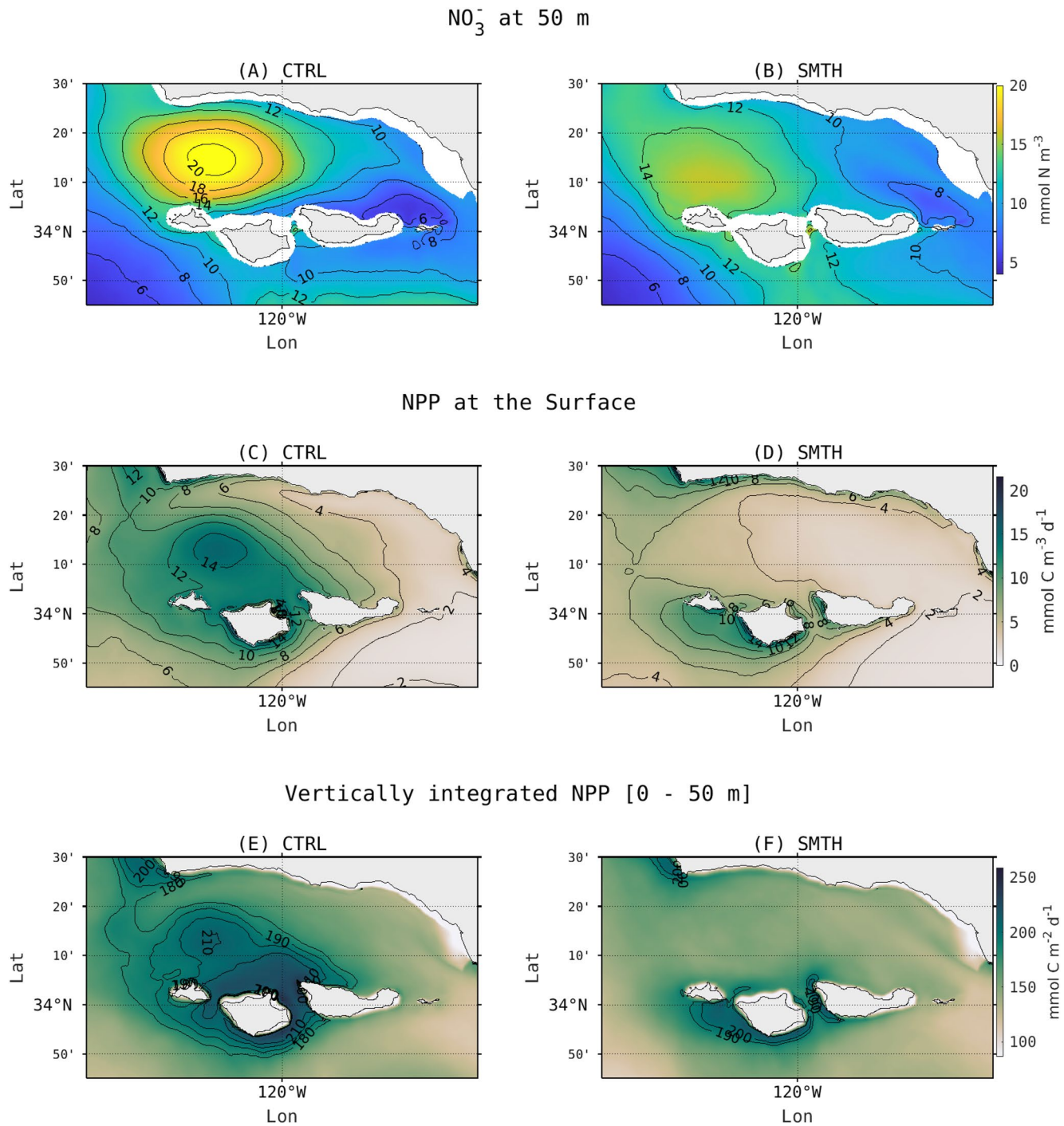


Figure 5. Color contours in (a) to (f) show the impact of low-level wind resolution on: nitrate concentration at 50 m depth in (a), (b) on surface net primary production in (c), (d), and integrated net primary production in (e), (f). Values are shown for summertime (1 June to 31 August 2000). In (k) and (l), black dashed lines show potential density.

biomass are highly correlated ($R^2 = 0.79$, $p < 0.01$). Similar to upwelling, eddy kinetic energy and vorticity also show a seasonal maximum between spring and summer, when submesoscale eddy activity and the associated nutrient delivery to the surface also peak, and are characterized by more intense high frequency pulses of phytoplankton biomass.

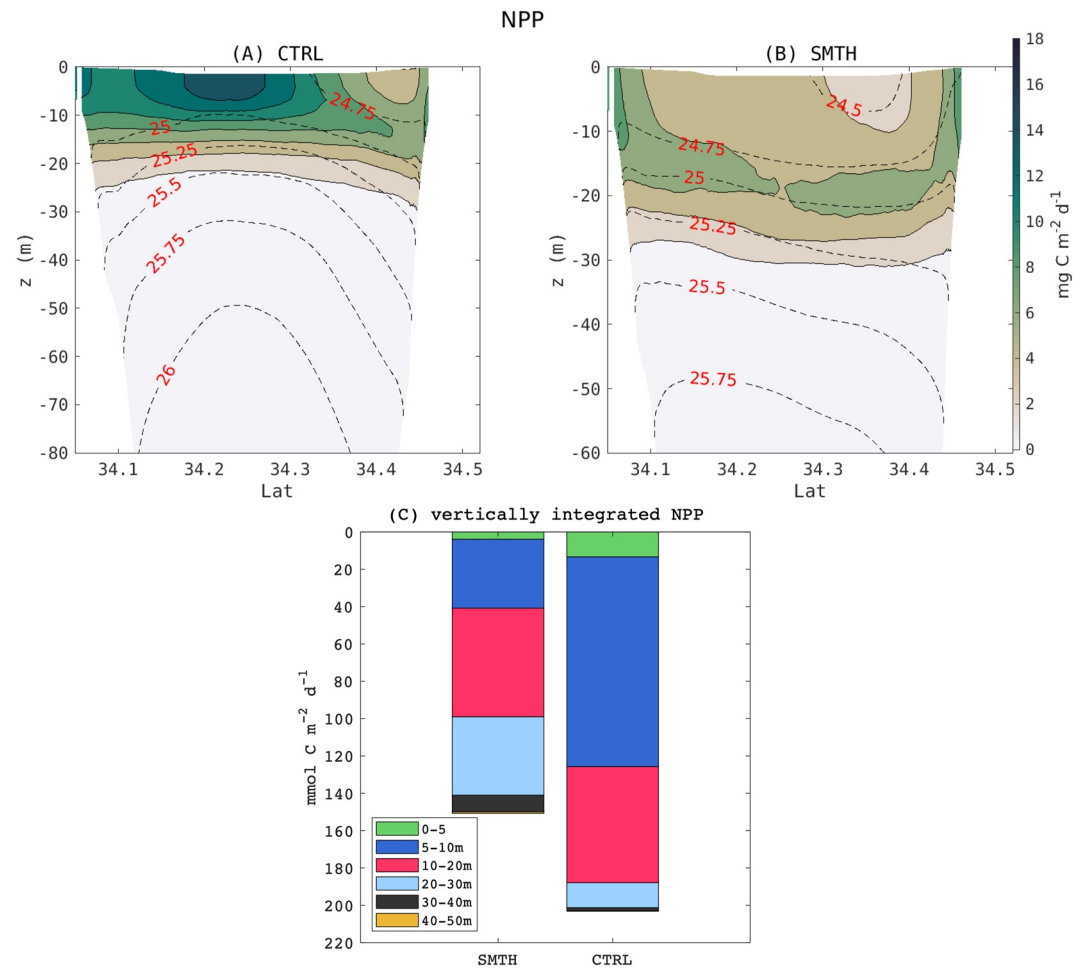


Figure 6. (a) and (b) show the net primary production along a vertical section crossing the Channel shown by the red line in Figure 1a, for CTRL and SMTH respectively. (c) Vertically integrated net primary production in CTRL and SMTH by vertical layer in average in the center of Santa Barbara channel.

3.3. Effects on Oxygen and Carbon

Oxygen and carbon system parameters, including pH, have been shown to respond rapidly to upwelling in the California Current (Chan et al., 2019). The average oxygen concentration near the center of the SBC at 50 m depth is 190 mmol m^{-3} during the period 1997–2000 in the CTRL case, with a variability of the order of 40 mmol m^{-3} , maximum values in winter ($\sim 250 \text{ mmol m}^{-3}$), and minimum values in summer ($\sim 100 \text{ mmol m}^{-3}$) (Figure 7). While the majority of this variability occurs on seasonal timescales, and can be attributed to seasonal upwelling, about 25 mmol m^{-3} (the residual after applying a 90-day moving average) are caused by submesoscale eddies that occur near the center of the Channel (Figure 7). Occasionally, these eddies can reduce oxygen concentrations by more than 100 mmol m^{-3} pH follows a nearly identical seasonal cycle, with a seasonal reduction of up to 0.15 between spring and summer, and an average variability of 0.1 caused by eddies (Figure 7).

As an example of impacts, we consider the effect of these eddies on the aerobic habitat of northern anchovy (*Engraulis mordax*), an ecologically important epipelagic species endemic to the CCS, using a Metabolic Index approach (Deutsch et al., 2021; Howard et al., 2020). The lowest values of O_2 simulated inside the eddies at 50 m reach about $100 \text{ O}_2 \text{ mmol m}^{-3}$. For a temperature of 8.5 C this corresponds to a Metabolic Index (ϕ) for northern anchovy of 2.68, which is well below the critical value ($\phi = 3$) for this species (Howard et al., 2020), suggesting a potential habitat reduction driven by the eddies. Similarly, for a pH of 7.8, and omega aragonite of 0.72 which is below the lethal limit for pteropods (Bednaršek et al., 2017), one ecologically important species in the CCS, suggesting a potential habitat compression for this species.

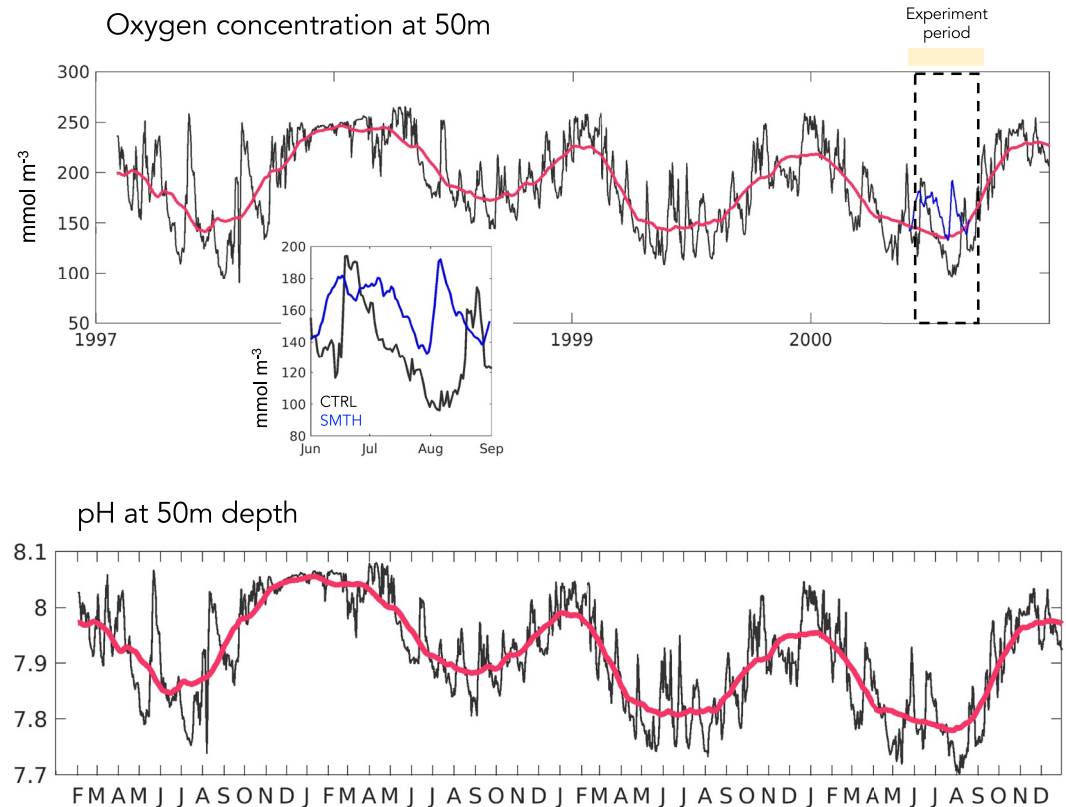


Figure 7. Time-series of oxygen and pH at 50 m depth. Black line is daily outputs, red line a smoothing average with 90 days window. The small box in the upper panel compares the concentration between CTRL and SMTH during the summertime experiment. Red line shows the seasonal variability and the fluctuations in black line expresses the effects of the mesoscale and submesoscale eddies.

The presence of intense submesoscale eddies tends to reduce oxygen concentrations near the center of the SBC (Figures 8a and 8b), by the same mechanism of upward doming and outcrop of deep, oxygen-poor isopycnals discussed in Section 3.2. Because these eddies often leave the Channel to travel northwest, their biogeochemical imprint can be felt further offshore in adjacent waters of the CCS. For example, by bringing deep, low oxygen, and low pH waters near the surface, and redistributing them away from the Channel, they act to reduce mean oxygen and pH over a broader region, generating small-scale, intense, albeit transient “hot spots” of low oxygen, low pH waters in otherwise more oxygenated and less acidic waters (similar to the mechanisms discussed in Frenger et al. (2018)).

The spatial extent of this influence is illustrated in Figure 8c, which shows the minimum subsurface oxygen concentration over the decade between 1997 and 2007, based on the longer 1 km-resolution simulation. Tracking these cyclonic, low-oxygen eddies as they leave the channel and are entrained in the California Current, reveals their characteristic structure illustrated in Figure 8d. The core of typical eddies has a diameter of the order of ~20 km, and they carry a low-oxygen, low-pH signature that deepens progressively over scales of weeks to months, as the eddies subduct underneath offshore waters (Figure 8d–8f). A caveat of the results shown in Figure 8c is that eddy features in the 1-km simulation are somewhat less intense than in the 300 m simulation, owing to the limited ability to resolve submesoscale dynamics (Kessouri, Bianchi, et al., 2020). Thus, these results should be taken as conservative estimates of the strength of submesoscale eddy effects on biogeochemistry.

4. Discussion and Conclusions

In this paper, we analyze the drivers and consequences of intense submesoscale cyclonic eddies generated by the island mass effect in the SBC. The strength of these eddies is modulated by two co-occurring air-sea-land interactions. The mechanical interaction between surface currents and surface stress causes a transfer of energy

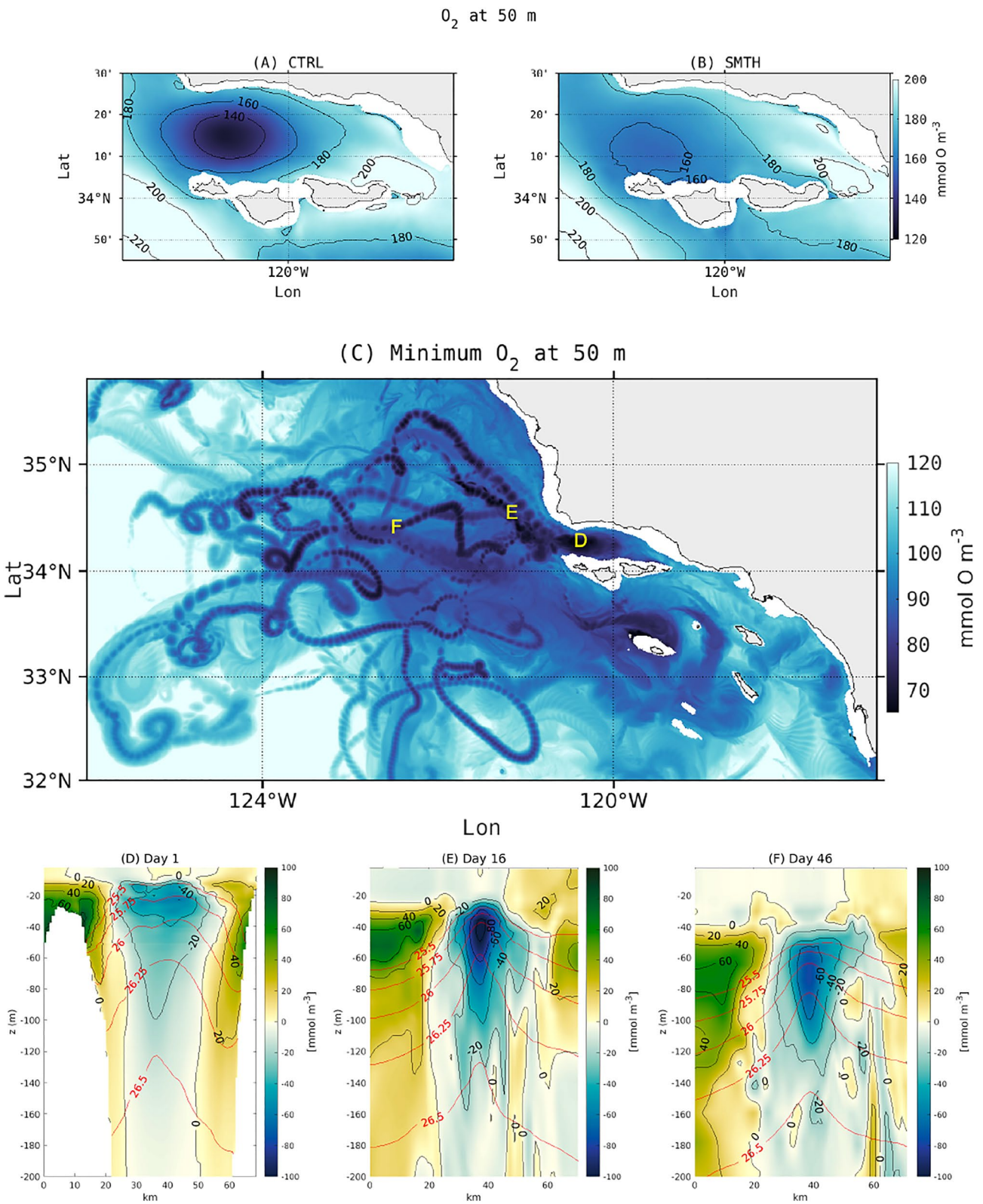


Figure 8.

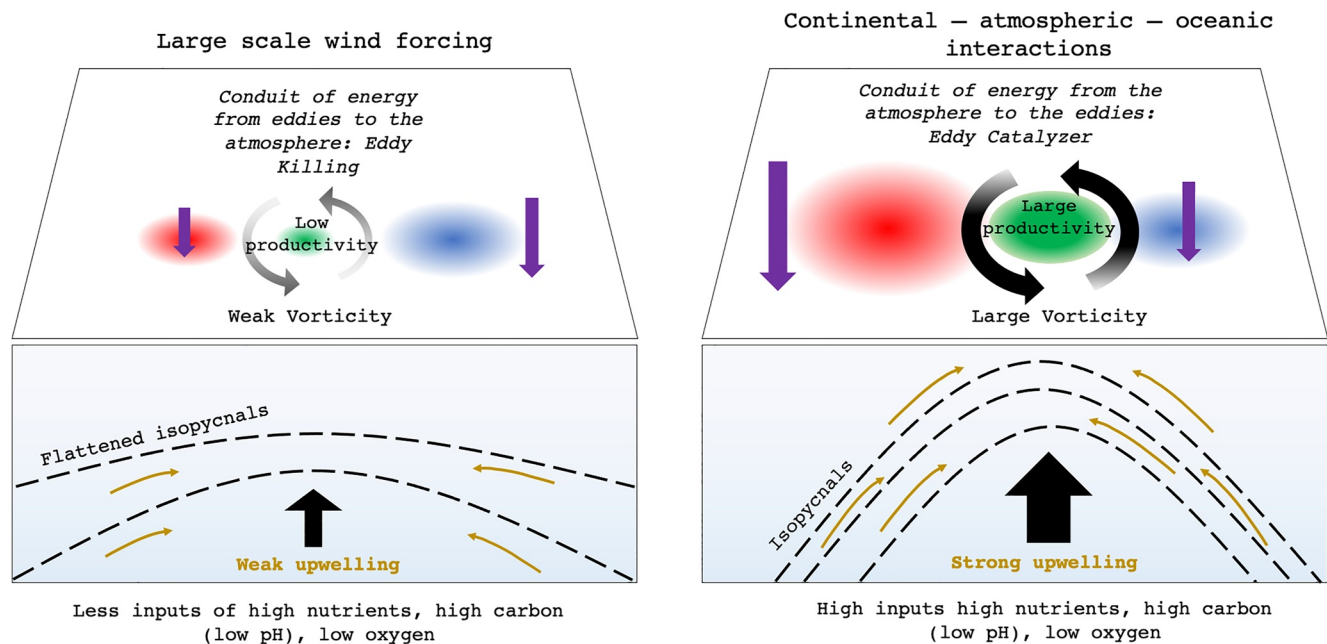


Figure 9. Schematic of coupled air-sea-land interactions leading to strengthening of submesoscale cyclonic eddies in the Santa Barbara Channel in spring and summer. The green circular shading represents ocean productivity, and is surrounded by curved black arrows representing the intensity of the eddy vorticity near the center of the Channel. The size of the red and blue circular shadings show the intensity of the windwork; red is a conduit of energy to the ocean, and blue is a conduit of energy to the atmosphere. The purple arrows schematize the intensity of the wind curl. Dashed black lines illustrate doming isopycnal surfaces, and shoaling of the nutricline and of oxygen and pH isosurfaces. Yellow arrows illustrate upwelling of deep waters along isopycnals. High vorticity strengthens the upward doming of isopycnals, pumping nutrient-rich, low-oxygen, low-pH waters toward the surface, thus enhancing phytoplankton productivity.

from the oceanic currents to the atmosphere, which dampens submesoscale activity (by *eddy killing*). However, in the SBC, this effect is overwhelmed by fine-scale wind patterns induced by the presence of surrounding capes and islands. These fine-scale winds cause an additional conduit of energy from the atmosphere to the ocean that eventually energizes submesoscale eddies (see schematic in Figure 9).

As in other upwelling systems, net primary production in the SBC is mainly driven by seasonal wind-driven upwelling that bring deep, nutrient-rich waters to the surface. However, this effect is reinforced by the intensification of submesoscale eddies, which cause an upward doming of isopycnals near the center of the Channel, increasing nutrient delivery to the surface. This in turn triggers intense phytoplankton blooms that enhance productivity and alter the ecosystem structure of the Channel.

Our simulations suggest that, in the absence of fine-scale winds, the region would be likely more similar to the rest of the Southern California Bight, with more typical oligotrophic conditions, nutrient and chlorophyll-depleted surface waters, subsurface chlorophyll maxima, and smaller phytoplankton cell size. In contrast, in the presence of fine-scale winds, the systems shifts toward more typical mesotrophic conditions, characterized by high surface net primary production, high organic matter export, and larger phytoplankton size. This in turn could favor the occurrence of harmful algal blooms by the toxin-producing diatom genus *Pseudo-nitzschia*, which are often observed in the region (Anderson et al., 2006).

Lastly, we show that a more pronounced isopycnal doming caused by wind-intensified submesoscale cyclones has consequences on oxygen and carbon in the SBC and beyond. Submesoscale eddies pump deep, oxygen-poor, acidic waters at the center of the Channel. These waters are then transported away from the Channel into the broader California Current, and can therefore impact a wider area by decreasing mean surface oxygen and pH,

Figure 8. Impact of low-level wind resolution and submesoscale cyclonic eddies on oxygen concentration. (a) and (b) show a comparison of summertime (June 1st to 31 August 2000) subsurface oxygen concentration (50 m) between CTRL (a) and SMTH (b). (c) shows the minimum oxygen concentration at 50 m between 01/1997 and 12/2007 from a 1 km-resolution simulation. Eddies generated inside the Channel spread Northwest and subduct in the California Current System, as shown by the low-oxygen eddy tracks. (d)–(f) Vertical sections crossing submesoscale cyclonic eddies inside the Channel (d), after 16 days, about 150 km north west of the Channel (e), and after 46 days, about 250 km west of the Channel (f). Color contours in (d)–(f) show oxygen anomalies relative to the surrounding waters (calculated by subtracting the mean oxygen profile along the sections), and red lines isopycnal surfaces.

and increasing the frequency of low-oxygen, low-pH events. While an analogous effect had been documented for submesoscale anticyclones (Frenger et al., 2018; Lukas & Santiago-Mandujano, 2001), this is to our knowledge the first time it is documented for submesoscale cyclones. Presence of eddies with anomalously low oxygen and pH could in turn contribute to compressing the habitat of pelagic species that are sensitive to low-oxygen, acidic waters (Bednaršek et al., 2017; Howard et al., 2020). Submesoscale-resolving numerical simulations are optimally suited to investigate the impacts of the SBC eddies and similar sources of fine-scale variability on pelagic communities in the California Current System.

Data Availability Statement

Code is available in Kessouri, McWilliams, et al. (2020) (10.5281/zenodo.6886319). Local land-based and atmospheric data can be found in Sutula et al. (2021) (doi: 10.5281/zenodo.4448224). Due to the size of output, model outputs are available from the Authors upon request.

Acknowledgments

This research was supported by the National Oceanic and Atmospheric Administration under grants for ocean acidification NA15NOS4780186, California Ocean Protection Council Grant C0100400. This work was supported by National Oceanic and Atmospheric Administration under ECOHAB award NA18NOS4780174. Computational resources were provided by the Extreme Science and Engineering Discovery Environment (XSEDE) through allocation TG-OCE170017, and by the super-computer Hoffman2 at the University of California Los Angeles, at the Institute for Digital Research and Education (IDRE, UCLA).

References

- Anderson, C. R., Brzezinski, M. A., Washburn, L., & Kudela, R. (2006). Circulation and environmental conditions during a toxigenic pseudo-nitzschia Australis bloom in the Santa Barbara Channel, California. *Marine Ecology Progress Series*, 327, 119–133. <https://doi.org/10.3354/meps327119>
- Bednaršek, N., Feely, R., Tolimieri, N., Hermann, A., Siedlecki, S., Waldbusser, G., et al. (2017). Exposure history determines pteropod vulnerability to ocean acidification along the US west coast. *Scientific Reports*, 7(1), 1–12. <https://doi.org/10.1038/s41598-017-03934-z>
- Brzezinski, M. A., & Washburn, L. (2011). Phytoplankton primary productivity in the Santa Barbara Channel: Effects of wind-driven upwelling and mesoscale eddies. *Journal of Geophysical Research*, 116(C12), C12013. <https://doi.org/10.1029/2011jc007397>
- Bye, J. A. (1985). Large-scale momentum exchange in the coupled atmosphere-ocean. *Elsevier Oceanography Series*, 40, 51–61. [https://doi.org/10.1016/s0422-9894\(08\)70702-5](https://doi.org/10.1016/s0422-9894(08)70702-5)
- Caldeira, R., Groom, S., Miller, P., Pilgrim, D., & Neelin, N. (2002). Sea-surface signatures of the island mass effect phenomena around Madeira island, northeast Atlantic. *Remote Sensing of Environment*, 80(2), 336–360. [https://doi.org/10.1016/s0034-4257\(01\)00316-9](https://doi.org/10.1016/s0034-4257(01)00316-9)
- Caldeira, R. M., Marchesiello, P., Neelin, N. P., DiGiacomo, P. M., & McWilliams, J. C. (2005). Island wakes in the southern California bight. *Journal of Geophysical Research*, 110(C11), C11012. <https://doi.org/10.1029/2004jc002675>
- Chan, F., Barth, J. A., Kroeker, K. J., Lubchenco, J., Menge, B. A., & Menge, B. (2019). The dynamics and impact of ocean acidification and hypoxia. *Oceanography*, 32(3), 62–71. <https://doi.org/10.5670/oceanog.2019.312>
- Chelton, D. (2001). *Report of the high-resolution ocean topography science working group meeting*. Oregon State University, College of Oceanic and Atmospheric Sciences.
- Chelton, D. B., Schlax, M. G., Freilich, M. H., & Milliff, R. F. (2004). Satellite measurements reveal persistent small-scale features in ocean winds. *Science*, 303(5660), 978–983. <https://doi.org/10.1126/science.1091901>
- Chelton, D. B., Schlax, M. G., Samelson, R. M., & De Szoeke, R. A. (2007). Global observations of large oceanic eddies. *Geophysical Research Letters*, 34(15). <https://doi.org/10.1029/2007gl030812>
- Chelton, D. B., & Xie, S.-P. (2010). Coupled ocean-atmosphere interaction at oceanic mesoscales. *Oceanography*, 23(4), 52–69. <https://doi.org/10.5670/oceanog.2010.05>
- Chen, R., McWilliams, J. C., & Renault, L. (2021). Momentum governors of California undercurrent transport. *Journal of Physical Oceanography*, 51(9), 2915–2932. <https://doi.org/10.1175/jpo-d-20-0234.1>
- Deutsch, C., Frenzel, H., McWilliams, J. C., Renault, L., Kessouri, F., Howard, E., et al. (2021). Biogeochemical variability in the California current system. *Progress in Oceanography*, 196, 102565. <https://doi.org/10.1016/j.pocean.2021.102565>
- Dewar, W. K., & Flierl, G. R. (1987). Some effects of the wind on rings. *Journal of Physical Oceanography*, 17(10), 1653–1667. [https://doi.org/10.1175/1520-0485\(1987\)017<1653:seotwo>2.0.co;2](https://doi.org/10.1175/1520-0485(1987)017<1653:seotwo>2.0.co;2)
- Dong, C., & McWilliams, J. C. (2007). A numerical study of island wakes in the southern California bight. *Continental Shelf Research*, 27(9), 1233–1248. <https://doi.org/10.1016/j.csr.2007.01.016>
- Dong, C., McWilliams, J. C., & Shepetchkin, A. F. (2007). Island wakes in deep water. *Journal of Physical Oceanography*, 37(4), 962–981. <https://doi.org/10.1175/jpo3047.1>
- Doty, M. S., & Oguri, M. (1956). The island mass effect. *ICES Journal of Marine Science*, 22(1), 33–37. <https://doi.org/10.1093/icesjms/22.1.33>
- Duhaut, T. H., & Straub, D. N. (2006). Wind stress dependence on ocean surface velocity: Implications for mechanical energy input to ocean circulation. *Journal of Physical Oceanography*, 36(2), 202–211. <https://doi.org/10.1175/jpo2842.1>
- Eilers, P. H. (2003). A perfect smoother. *Analytical Chemistry*, 75(14), 3631–3636. <https://doi.org/10.1021/ac034173t>
- Fairall, C. W., Bradley, E. F., Hare, J., Grachev, A. A., & Edson, J. B. (2003). Bulk parameterization of air–sea fluxes: Updates and verification for the coare algorithm. *Journal of Climate*, 16(4), 571–591. [https://doi.org/10.1175/1520-0442\(2003\)016<0571:bpoasf>2.0.co;2](https://doi.org/10.1175/1520-0442(2003)016<0571:bpoasf>2.0.co;2)
- Frenger, I., Bianchi, D., Stührenberg, C., Oschlies, A., Dunne, J., Deutsch, C., et al. (2018). Biogeochemical role of subsurface coherent eddies in the ocean: Tracer cannonballs, hypoxic storms, and microbial stewpots? *Global Biogeochemical Cycles*, 32(2), 226–249. <https://doi.org/10.1002/2017gb005743>
- Hendershott, M., & Winant, C. (1996). Surface circulation in the Santa Barbara Channel. *Oceanography*, 9(2), 114–121. <https://doi.org/10.5670/oceanog.1996.14>
- Howard, E. M., Penn, J. L., Frenzel, H., Seibel, B. A., Bianchi, D., Renault, L., et al. (2020). Climate-driven aerobic habitat loss in the California current system. *Science Advances*, 6(20), eaay3188. <https://doi.org/10.1126/sciadv.aay3188>
- Ioannou, A., Stegner, A., Dubos, T., Le Vu, B., & Speich, S. (2020). Generation and intensification of mesoscale anticyclones by orographic wind jets: The case of Ierapetra eddies forced by the Etesians. *Journal of Geophysical Research: Oceans*, 125(8), e2019JC015810. <https://doi.org/10.1029/2019jc015810>

- Kessouri, F., Bianchi, D., Renault, L., McWilliams, J. C., Frenzel, H., & Deutsch, C. A. (2020). Submesoscale currents modulate the seasonal cycle of nutrients and productivity in the California current system. *Global Biogeochemical Cycles*, *34*(10), e2020GB006578. <https://doi.org/10.1029/2020gb006578>
- Kessouri, F., McLaughlin, K., Sutula, M., Bianchi, D., Ho, M., McWilliams, J. C., et al. (2021). Configuration and validation of an oceanic physical and biogeochemical model to investigate coastal eutrophication in the southern California bight. *Journal of Advances in Modeling Earth Systems*, *13*(12), e2020MS002296. <https://doi.org/10.1029/2020ms002296>
- Kessouri, F., McLaughlin, K., Sutula, M., Ho, M., McWilliams, J. C., & Bianchi, D. (2020). Collection of in situ monitoring data in the Southern California Bight 1950–2017 for model validation. *Zenodo*. <https://doi.org/10.5281/zenodo.4536641>
- Kessouri, F., McWilliams, C. J., Deutsch, C., Renault, L., Frenzel, H., Bianchi, D., & Molemaker, J. (2020). ROMS-BEC oceanic physical and biogeochemical model code for the Southern California current system V2020. *Zenodo*. <https://doi.org/10.5281/zenodo.3988618>
- Kuhn, C. E., & Costa, D. P. (2014). Interannual variation in the at-sea behavior of California sea lions (*Zalophus californianus*). *Marine Mammal Science*, *30*(4), 1297–1319. <https://doi.org/10.1111/mms.12110>
- Lukas, R., & Santiago-Mandujano, F. (2001). Extreme water mass anomaly observed in the Hawaii ocean time-series. *Geophysical Research Letters*, *28*(15), 2931–2934. <https://doi.org/10.1029/2001gl013099>
- Ma, X., Jing, Z., Chang, P., Liu, X., Montuoro, R., Small, R. J., et al. (2016). Western boundary currents regulated by interaction between ocean eddies and the atmosphere. *Nature*, *535*(7613), 533–537. <https://doi.org/10.1038/nature18640>
- Mahadevan, A., & Archer, D. (2000). Modeling the impact of fronts and mesoscale circulation on the nutrient supply and biogeochemistry of the upper ocean. *Journal of Geophysical Research*, *105*(C1), 1209–1225. <https://doi.org/10.1029/1999jc900216>
- McGillicuddy, D. J., Jr. (2016). Mechanisms of physical-biological-biogeochemical interaction at the oceanic mesoscale. <https://doi.org/10.1146/annurev-marine-010814-015606>
- Messié, M., Petrenko, A., Doglioli, A. M., Aldebert, C., Martinez, E., Koenig, G., et al. (2020). The delayed island mass effect: How islands can remotely trigger blooms in the oligotrophic ocean. *Geophysical Research Letters*, *47*(2), e2019GL085282. <https://doi.org/10.1029/2019gl085282>
- Minobe, S., Kuwano-Yoshida, A., Komori, N., Xie, S.-P., & Small, R. J. (2008). Influence of the gulf stream on the troposphere. *Nature*, *452*(7184), 206–209. <https://doi.org/10.1038/nature06690>
- Moore, J. K., Doney, S. C., & Lindsay, K. (2004). Upper ocean ecosystem dynamics and iron cycling in a global three-dimensional model. *Global Biogeochemical Cycles*, *18*(4). <https://doi.org/10.1029/2004gb002220>
- O'Neill, L. W. (2012). Wind speed and stability effects on coupling between surface wind stress and SST observed from buoys and satellite. *Journal of Climate*, *25*(5), 1544–1569. <https://doi.org/10.1175/jcli-d-11-00121.1>
- O'Neill, L. W., Esbensen, S. K., Thum, N., Samelson, R. M., & Chelton, D. B. (2010). Dynamical analysis of the boundary layer and surface wind responses to mesoscale SST perturbations. *Journal of Climate*, *23*(3), 559–581. <https://doi.org/10.1175/2009jcli2662.1>
- Renault, L., Deutsch, C., McWilliams, J. C., Frenzel, H., Liang, J.-H., & Colas, F. (2016). Partial decoupling of primary productivity from upwelling in the California current system. *Nature Geoscience*, *9*(7), 505–508. <https://doi.org/10.1038/ngeo2722>
- Renault, L., Hall, A., & McWilliams, J. C. (2016). Orographic shaping of U.S. West coast wind profiles during the upwelling season. *Climate Dynamics*, *46*(1–2), 1–17. <https://doi.org/10.1007/s00382-015-2583-4>
- Renault, L., Marchesiello, P., Masson, S., & McWilliams, J. C. (2019). Remarkable control of Western boundary currents by eddy killing, a mechanical air-sea coupling process. *Geophysical Research Letters*, *46*(5), 2743–2751. <https://doi.org/10.1029/2018gl081211>
- Renault, L., Masson, S., Arsouze, T., Madec, G., & McWilliams, J. C. (2020). Recipes for how to force oceanic model dynamics. *Journal of Advances in Modeling Earth Systems*, *12*(2). <https://doi.org/10.1029/2019ms001715>
- Renault, L., Masson, S., Oerder, V., Jullien, S., & Colas, F. (2019). Disentangling the mesoscale ocean-atmosphere interactions. *Journal of Geophysical Research: Oceans*, *124*(3), 2164–2178. <https://doi.org/10.1029/2018jc014628>
- Renault, L., McWilliams, J. C., & Gula, J. (2018). Dampening of submesoscale currents by air-sea stress coupling in the Californian upwelling system. *Scientific Reports*, *8*(1), 1–8. <https://doi.org/10.1038/s41598-018-31602-3>
- Renault, L., McWilliams, J. C., Kessouri, F., Jousse, A., Frenzel, H., Chen, R., & Deutsch, C. (2021). Evaluation of high-resolution atmospheric and oceanic simulations of the California current system. *Progress in Oceanography*, *195*, 102564. <https://doi.org/10.1016/j.pocean.2021.102564>
- Renault, L., McWilliams, J. C., & Masson, S. (2017). Satellite observations of imprint of oceanic current on wind stress by air-sea coupling. *Scientific Reports*, *7*(1), 1–7. <https://doi.org/10.1038/s41598-017-17939-1>
- Renault, L., Molemaker, M. J., McWilliams, J. C., Shchepetkin, A. F., Lemarié, F., Chelton, D., et al. (2016). Modulation of wind work by oceanic current interaction with the atmosphere. *Journal of Physical Oceanography*, *46*(6), 1685–1704. <https://doi.org/10.1175/jpo-d-15-0232.1>
- Seo, H., Miller, A. J., & Norris, J. R. (2016). Eddy–wind interaction in the California current system: Dynamics and impacts. *Journal of Physical Oceanography*, *46*(2), 439–459. <https://doi.org/10.1175/jpo-d-15-0086.1>
- Shchepetkin, A. F. (2015). An adaptive, courant-number-dependent implicit scheme for vertical advection in oceanic modeling. *Ocean Modelling*, *91*, 38–69. <https://doi.org/10.1016/j.ocemod.2015.03.006>
- Shchepetkin, A. F., & McWilliams, J. C. (2005). The regional oceanic modeling system (roms): A split-explicit, free-surface, topography-following-coordinate oceanic model. *Ocean Modelling*, *9*(4), 347–404. <https://doi.org/10.1016/j.ocemod.2004.08.002>
- Skamarock, W. C., & Klemp, J. B. (2008). A time-split nonhydrostatic atmospheric model for weather research and forecasting applications. *Journal of Computational Physics*, *227*(7), 3465–3485. <https://doi.org/10.1016/j.jcp.2007.01.037>
- Sutula, M., Ho, M., Sengupta, A., Kessouri, F., McLaughlin, K., McCune, K., & Bianchi, D. (2021). A baseline of terrestrial freshwater and nitrogen fluxes to the southern California bight, USA. *Zenodo*, *170*, 112669. <https://doi.org/10.1016/j.marpolbul.2021.112669>
- Winant, C., Dorman, C., Friehe, C., & Beardsley, R. (1988). The marine layer off northern California: An example of supercritical channel flow. *Journal of the Atmospheric Sciences*, *45*(23), 3588–3605. [https://doi.org/10.1175/1520-0469\(1988\)045<3588:tmlonc>2.0.co;2](https://doi.org/10.1175/1520-0469(1988)045<3588:tmlonc>2.0.co;2)